Vol 16 No 3, March 2007
1009-1963/2007/16(03)/0700-07

Chinese Physics

© 2007 Chin. Phys. Soc.
and IOP Publishing Ltd

Ab initio calculations for the absorption spectra and polarizabilities of small sulfur clusters*

Bai Yu-Lin(白玉林)[a], Chen Xiang-Rong(陈向荣)[b]†,
Cheng Xiao-Hong(程晓洪)[a], and Yang Xiang-Dong(杨向东)[a,b]

[a] *Department of Physics and Electronic Information, Yibin University, Yibin* 644000, *China*

[b] *Institute of Atomic and Molecular Physics, Sichuan University, Chengdu* 610065, *China*

(Received 4 June 2006; revised manuscript received 12 September 2006)

Absorption spectra for S_n clusters ($n = 2 \ldots 8$) are calculated using an adiabatic time-dependent density functional formalism within the local density approximation (LDA). We compare the calculated spectra with those computed using a simple LDA approach. The time-dependent LDA (TDLDA) spectra display a significant blue shift with respect to the LDA spectra. The calculated spectra present a variety of features that can be used for comparison with future experimental investigations. We also obtain a significant threshold absorption, which can distinguish between different ground states of the sulfur clusters. In addition, the polarizabilities of the clusters are calculated by using the higher-order finite-difference pseudopotential density functional method in real space. We find that the polarizabilities of the clusters considered are higher than the value estimated from the 'hard sphere' model using the bulk static dielectric constant. The computed polarizabilities per atom tend to decrease with increasing cluster size. The polarizabilities are closely related to the HOMO–LUMO gaps and the geometrical configurations.

Keywords: absorption spectra, threshold absorption, polarizability, HOMO–LUMO gaps
PACC: 3640C, 3120J, 3365C, 3520M

1. Introduction

Owing to their unusual electronic and structural properties, clusters have received considerable attention. There were many theoretical approaches to predict the most stable structure of small cluster, but different theories favour different geometries even for the same cluster.[1−3] Sulfur occurs in more allotropic forms than any other elements in the periodic table. It is known that the dimer S_2 has a triplet ground state. Though the small clusters S_{3-5} have been studied, their ground state geometric structures have not been experimentally determined directly. Detailed x-ray structures and vibrational spectroscopic information are available only for sulfur rings (S_n, $n = 6 \ldots 8$). There have been many theoretical studies on sulfur clusters, ranging from *ab initio* studies to Monte Carlo approaches.[4−19]

Unfortunately, not all these results could be compared with experimental data. One experiment that can be performed with clusters is the measurement of their absorption spectra. Such measurements have been reported previously for alkali metal clusters, e.g., Li[20] and Na,[21] and for well-known semiconductors, e.g., Si and GaAs.[22,23] Therefore, theoretical calculations of the optical spectra for clusters are of particular importance, because they can be directly compared with experiments. However, this inherently involves the calculation of excited-state properties, which is much more difficult. The configuration-interaction method[24] should allow for calculating absorption spectra. However, it is computationally intensive and usually limited to small molecules. Recently, it has been shown that a solution of the Bethe–Salpeter equation for the two-particle Green function within the GW (Green function G and the screened Coulomb interaction W) approximation yields good results in agreement with the experimental.[25] While not as computationally intensive as the configuration-interaction method, it is still difficult to extend to larger clusters.

*Project supported by the National Natural Science Foundation of China (Grant No 10274055), the Natural Science Foundation of Sichuan Education Bureau, China (Grant No 2004A181) and the Research Fund for the Doctoral Program of Yibin University, China (Grant No 2005B01).

†Corresponding author. E-mail: xrchen@126.com

A different approach is based on time-dependent density functional theory (TDDFT). Formally, this is an exact approach, whereas in practice it is approximate owing to the use of the local density approximation (LDA) instead of the exact spatial dependence, and an adiabatic approximation instead of the exact time dependence of the exchange-correlation functional.[26] The ensuing time-dependent LDA (TDLDA) technique requires a substantially smaller computational effort and is able to handle much larger clusters. This technique has been applied to Na, Si, and GaAs clusters and was found to yield results in good agreement with experimental results.[27−39] Troparevskr *et al*[37] applied the TDLDA to predicting absorption spectra for small Cd_nSe_n clusters with $n = 2 \ldots 8$.

The polarizability is another important quantity of clusters, which can provide some information of geometrical features of the clusters. Thus, comprehensively understanding the polarizabilities from theoretical calculations is also important in cluster science.

2. Calculation methods

We apply the TDLDA technique to calculating the optical absorption spectra of S_n clusters ($n = 2 \ldots 8$), in an attempt to provide theoretical data that can be tested directly with future experimental work. A detailed analysis of TDLDA theory has been given elsewhere.[26] We apply it to the frequency-space approach, in which the electronic transition energies V_n are obtained from the solution of the following eigenvalue problem:[26]

$$[\omega_{ij\sigma}^2 \delta_{ik}\delta_{jl}\delta_{\sigma\tau} + 2\sqrt{f_{ij\sigma}\omega_{ij\sigma}}K_{ij\sigma,kl\tau} \times \sqrt{f_{kl\tau}\omega_{kl\sigma}}]\boldsymbol{F}_n = \Omega_n^2 \boldsymbol{F}_n, \quad (1)$$

where

$$\omega_{ij\sigma} = \varepsilon_{j\sigma} - \varepsilon_{i\sigma}$$

are the Kohn–Sham transition energies, and

$$f_{ij\sigma} = n_{i\sigma} - n_{j\sigma}$$

are the differences between the occupation numbers in the ith and jth states. The eigenvectors $\boldsymbol{F}_n$ are related to the oscillator strength, and $K_{ij\sigma,kl\tau}$ is a coupling matrix given by

$$K = \iint \phi_{i\sigma}^*(\boldsymbol{r})\phi_{j\sigma}(\boldsymbol{r})\Big[\frac{1}{|\boldsymbol{r}-\boldsymbol{r}'|} + \frac{\delta v_\sigma^{\mathrm{xc}}(\boldsymbol{r})}{\delta\rho_\tau(\boldsymbol{r}')}\Big] \times \phi_{k\tau}(\boldsymbol{r}')\phi_{l\tau}^*(\boldsymbol{r}')\mathrm{d}\boldsymbol{r}\mathrm{d}\boldsymbol{r}', \quad (2)$$

where $\phi(\boldsymbol{r})$ is a Kohn–Sham wave function; i, j, σ; k, l, τ are the occupied states, unoccupied states, and spin indices, respectively; $\rho(\boldsymbol{r})$ is the Kohn–Sham charge density, and $v^{\mathrm{xc}}(\boldsymbol{r})$ is the LDA exchange–correlation.

Our computational technique is based on the higher-order finite difference pseudopotential method.[30] We use the local density approximation of Ceperely and Alder[31] and Troullier–Martins *ab initio* pseudopotentials[32] with a partial core correction. The solution proceeds in three parts: First, the Kohn–Sham energies and wave functions are found by means of a conventional ground state calculation. Second, the wave functions are used to construct the coupling matrix of Eq.(2). Third, the TDLDA eigenvalue equation, Eq.(1), is solved and the absorption spectrum constructed. All the three steps are performed using a real-space grid confined in a spherical domain.

In order to describe the polarizability in momentum space, we employ the plane-wave perturbation theory and evaluate the dielectric function on a spatial grid,[33] which requires a large number of bands to be included in the calculations and thus significantly increases the computing time. On the other hand, our calculations are performed in real space, where polarizability can be defined in a very straightforward way, and the associated computational work requires minimal effort.

We use a finite-field method[34,35] to calculate the polarizability. In real space, we can include an external electric field in the Hamiltonian simply by adding one extra term to the effective potential:

$$\Big(-\frac{\hbar^2\nabla^2}{2m} + V_{\mathrm{eff}}(\boldsymbol{r}) - e\boldsymbol{F}\cdot\boldsymbol{r}\Big)\phi_i(\boldsymbol{r}) = E\phi_i(\boldsymbol{r}), \quad (3)$$

where the effective potential $V_{\mathrm{eff}}(\boldsymbol{r})$ includes ionic, Hartree, and exchange–correlation terms, $\phi_i(\boldsymbol{r})$ is the one-electron pseudowavefunction, and $\boldsymbol{F}$ is the applied uniform electric field. From the solution of Eq.(1), we can determine the dipole moment and the total ground-state energy versus the applied electric field.

The polarizability is defined as

$$\alpha_{ij} = -\Big(\frac{\partial^2 E}{\partial F_i \partial F_j}\Big), \quad (i, j = x, y, z). \quad (4)$$

Using the finite difference expressions for the first and second derivatives, we can find the diagonal elements of the polarizability tensor α_{ii} from the dipole moment μ, or from the total energy $E(\boldsymbol{F})$ at $\boldsymbol{F} = 0$, and $\boldsymbol{F} = \pm\delta F_i$ applied along the ith axis. The value

normally measured in the experiments is the average polarizability given by

$$\langle\alpha\rangle = \frac{1}{3}(\alpha_{xx} + \alpha_{yy} + \alpha_{zz}).$$

Because of rotational invariance of the trace of the polarizability tensor, this value does not depend on the choice of the coordinate system.

3. Results and discussions

To determine the ground state structures, we use a grid spacing $h = 0.8$ a.u., and require at least 10 a.u. separation between the position of any atom and the spherical boundary. The choice of these parameters is justified by the fact that no significant changes in the value of the total energy and the interatomic forces are detected with further increase of the radius of the boundary sphere or decrease of the grid spacing. The ground state structures and geometrical parameters are shown in our previous work.[17]

For the TDLDA calculations, we have carefully tested for convergence of the computed excitation energies and associated absorption spectra with respect to the size of the spherical domain, the grid spacing, and the total number of electronic states included in the calculations. Convergence was obtained with a domain radius of 33 a.u., a grid spacing of 0.6 a.u., and the number of unoccupied Kohn–Sham orbitals, which was at least three times greater than the number of occupied ones. The calculated TDLDA absorption spectra (solid lines) are shown in Fig.1. Also given are the absorption spectra of the same clusters obtained from LDA (dashed lines). All spectra have been broadened using a Gaussian, in order to simulate the effect of a finite temperature, as well as finite resolution of an experiment. We have used a Gaussian width of 0.1 eV, which is a typical accuracy for optical absorption measurements.

It is readily observed that in all cases shown in Fig.1 the TDLDA spectra display a significant blue shift with respect to the Kohn–Sham eigenvalue spectra. The same trend was found for Ga_nAs_n[28] and Si_{2n} clusters,[29] and it is consistent with the well-known band gap underestimate of time-independent density functional theory (DFT). This implies that TDLDA works well for systems with a significant degree of ionicity. There are other qualitative similarities between the current results and those of GaAs and Si clusters: One can observe a variety of spectral shapes and peak positions for the different-size clusters, which implies that clusters of different sizes can often be distinguished based on their optical spectrum 'fingerprint'. Another similarity of sulfur clusters to III–V and IV–IV clusters is the long absorption tails found in the spectra. These tails, which extend deeply into the region of lower transition energies, are likely due to the existence of free surfaces in the clusters. Such a behaviour is absent in quantum dots that are passivated at the boundaries,[36] unlike the clusters studied in this work.

For computing the absorption edge versus cluster size, we take the absorption edge (defined as in Ref.[37]) as the energy threshold, below which the absorption is 2% of the total absorption. We note that the photo absorption gap is different from the gap between highest occupied molecular orbital (HOMO) and lowest unoccupied molecular orbital (LUMO), because the first allowed excitation is often too weak to be detected. For a meaningful comparison with experiment, we use the same empirical criterion employed in interpreting experimental data.

The absorption thresholds calculated from both the TDLDA and the LDA spectra are given in Fig.2, along with the HOMO–LUMO gap extracted from the LDA eigenvalues. For $n = 2 \ldots 4$, the figure illustrates that the LDA absorption threshold calculated from the 2% rule is appreciably larger than the HOMO–LUMO gap for all the clusters. This is because the oscillator strength computed by using LDA at the HOMO–LUMO transition may be quite small, pushing the effective (2%) threshold upwards in energy. For $n = 4 \ldots 8$, the LDA absorption threshold calculated from the 2% rule nearly equal the HOMO–LUMO gap for all the clusters. Even so, the time-independent LDA calculations consistently and severely underestimate the TDLDA photo-absorption thresholds. The latter is greater than the band gap of the bulk phase, as expected from the quantum size effect and observed for III–V and IV–IV clusters. Interestingly, even though the photo absorption thresholds calculated using TDLDA for the S_n clusters are larger than those found using LDA, they exhibit similar trends to the variation of LDA thresholds with increasing cluster size (see Fig.2).

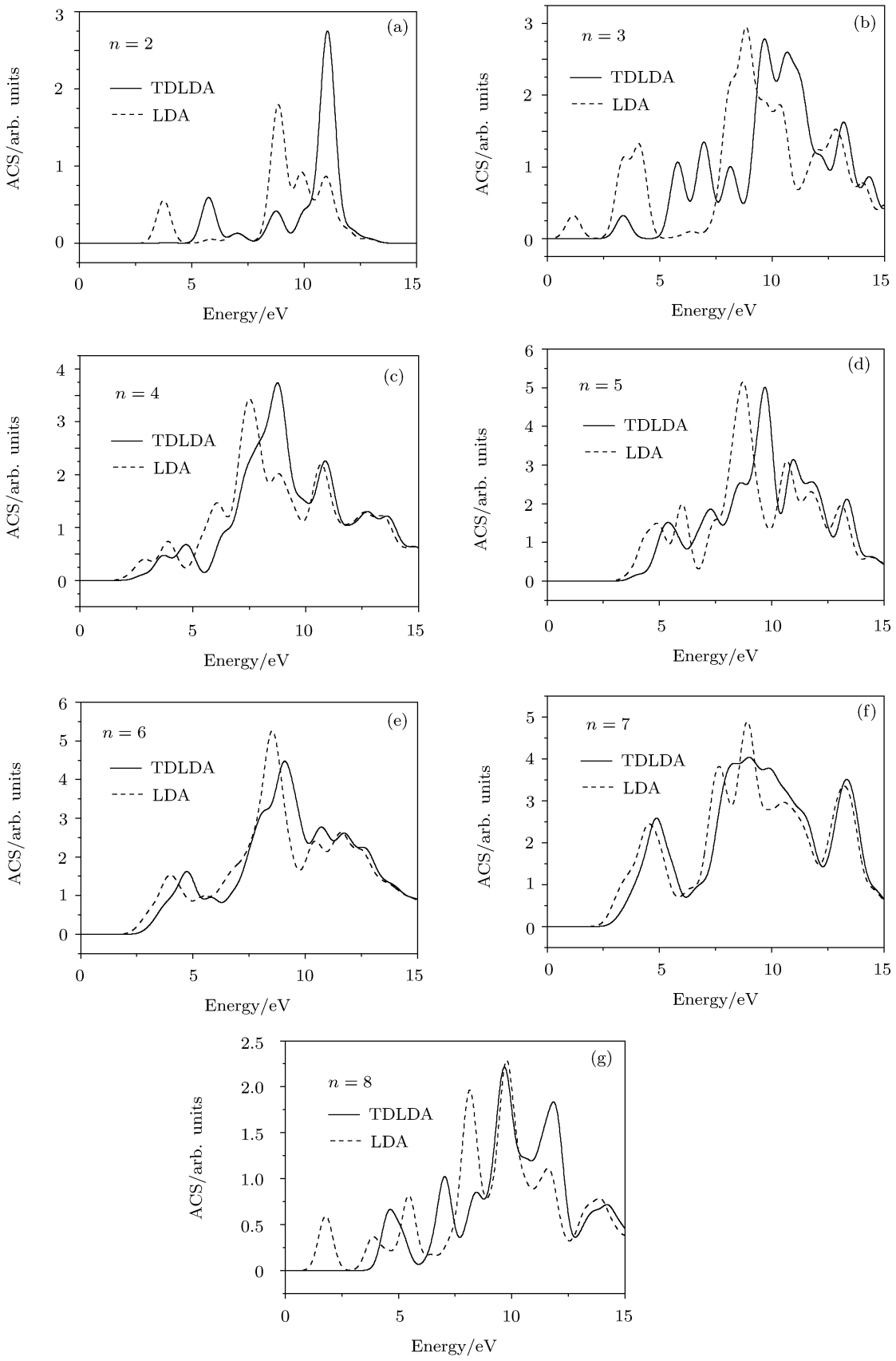


Fig.1. Calculated TDLDA (solid lines) and LDA (dashed lines) absorption of sulfur cluster. All spectra have been convoluted with an 0.1 eV wide Gaussian to simulate a finite broadening of the calculated spectra.

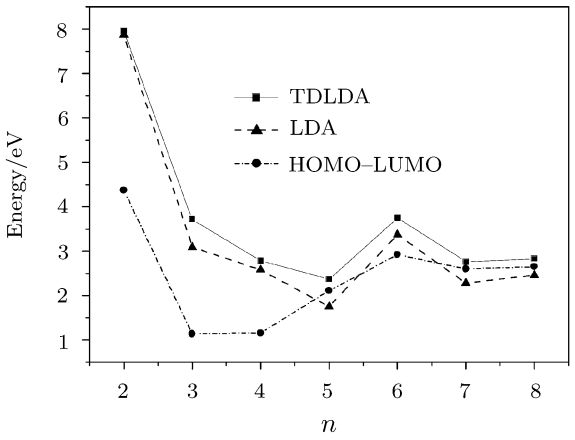


Fig.2. Calculated HOMO–LUMO gap and optical absorption thresholds. The solid lines, dashed lines and dotted lines are for TDLDA, LDA, and HOMO–LUMO, respectively.

We find that a larger spherical domain has to be included in the polarizability calculations other than that needed for the structural minimization. However, the computed polarizabilities are relatively insensitive to the size of the grid spacing. This behaviour agrees with the fact that polarizabilities mainly depend on the 'outer' part of the electron density of a cluster, whereas the 'inner' part is responsible for the bonding properties. Therefore, we use $h = 0.8$ a.u., and increase the radius of the boundary sphere up to 16 a.u. One of the most significant problems in the finite-field method is the choice of an appropriate field strength. In order to determine the stability of our calculations with respect to the magnitude of the applied electric field, we examine the influence of this parameter on the computed polarizabilities for several clusters. We find that the best region of linear response lies between $\delta F = 0.0001$ and 0.01 a.u., and within this range the values of polarizabilities are calculated from the total energy, and the dipole moment coincides with one another within 5%.

In Fig.3, we illustrate the calculated polarizabilities of S_2 as a function of the finite electric field. Under very low fields, the polarizabilities calculated by the change in dipole moment are not reliable because of numerical inaccuracies such as round off errors. In the case of very strong fields, the cluster can be ionized by the fields. However, for a wide range of values of the electric field, the calculated values are stable.

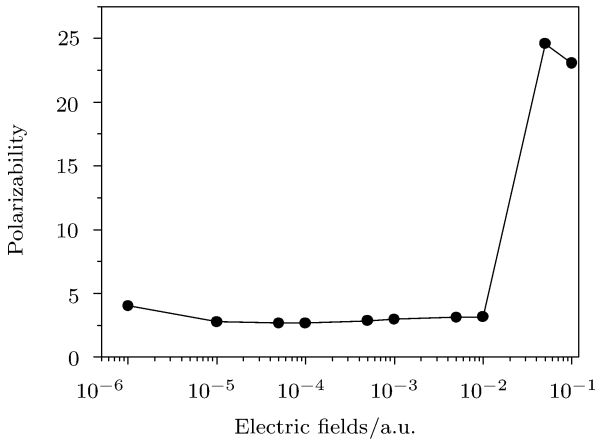


Fig.3. The polarizability (Å^3/atom) of S_2 as a function of the electric field.

Consequently, for all polarizability calculations we have chosen the external field δF to be 0.001 a.u. along x, y and z. We investigate the possible influence of relaxing ionic positions on polarizability in the finite field calculations. We find that including ionic relaxation does not affect the calculated polarizabilities within 5%.

Table 1. Static dipole moments (Debyes) and average polarizabilities (Å^3/atom) of sulfur clusters.

Cluster	Static dipole moments/Debyes	Average polarizabilities/(Å^3/atom)
S		2.87[a]
S_2	0	2.9661
S_3	0.7923	3.3783
S_4	0.0011	2.9906
S_5	0.0276	2.7188
S_6	1.1379	2.5878
S_7	1.2660	2.0271
S_8	0.0244	2.3237

[a]From Ref.[38].

Our results are listed in Table 1. The static dipole moments are computed by direct summation over all grid points at zero electric field. The listed data for polarizabilities are the average polarizabilities divided by the total number of atoms in the cluster. The polarizability of the single atom is taken from Ref.[38]. It is impossible for us to compare our results with experimental data because of the absence of any polarizability data on sulfur clusters. It is obvious that the polarizabilities of the clusters roughly equal those of single atoms. For S_2, S_3 and S_4, the polarizabilities of the clusters are higher than that of single atoms, whereas the polarizabilities of the other clusters are lower than those of single atoms.

The variation of the computed values for polarizabilities with the number of atoms in the cluster is shown in Fig.4(a). As a reference, we include the bulk limit for the polarizability, estimated from the Clausius–Mossotti relation:

$$\alpha = \frac{3}{4\pi}\frac{\varepsilon_{\rm b}-1}{\varepsilon_{\rm b}+2}v_{\rm at}, \tag{5}$$

where $v_{\rm at}$ is an elementary volume per atom in the crystalline state, and $\varepsilon_{\rm b}$ is the bulk dielectric constant. Equation (5) yields $\alpha = 1.91$ Å^3/atom. Figure 2(a) demonstrates that in all the cases our values are higher than the corresponding bulk, and the polarizabilities decrease with increasing size of the cluster.

We further discuss the relationship between the polarizability and the electronic structures of clusters. Figure 4(b) illustrates the polarizabilities as a function of the HOMO–LUMO energy gaps. As shown in Fig.4(b), the large polarizability generally corresponds to the small HOMO–LUMO gap. The clusters with $n = 2, 7$ have relatively smaller polarizabilities in comparison with their neighbouring size. For example, the HOMO–LUMO gap for S_7 is 2.60 eV and the polarizability is just 2.027 Å^3/atom. The polarizabilities decrease with the increase of the HOMO–LUMO gap as a whole. This can be easily rationalized using the two-level model[39]

$$\alpha \approx \frac{\mu_{\rm t}^2}{\Delta_{\rm t}}, \tag{6}$$

where $\mu_{\rm t}^2$ is the transition dipole moment from the ground state to the first dipole-allowed excited state and $\Delta_{\rm t}$ is the corresponding transition energy. Approximately, $\Delta_{\rm t}$ can be replaced with the HOMO–LUMO energy gap Δ. From this model, α increases with decreasing Δ, consistent with our calculated trend for most S_n clusters. However, α is not a simply inverse proportion relation to Δ, since the two quantities are dependent on each other. Small Δ tends to generate large $\mu_{\rm t}^2$. In addition, $\mu_{\rm t}^2$ depends on some other characters, such as the selection rule.

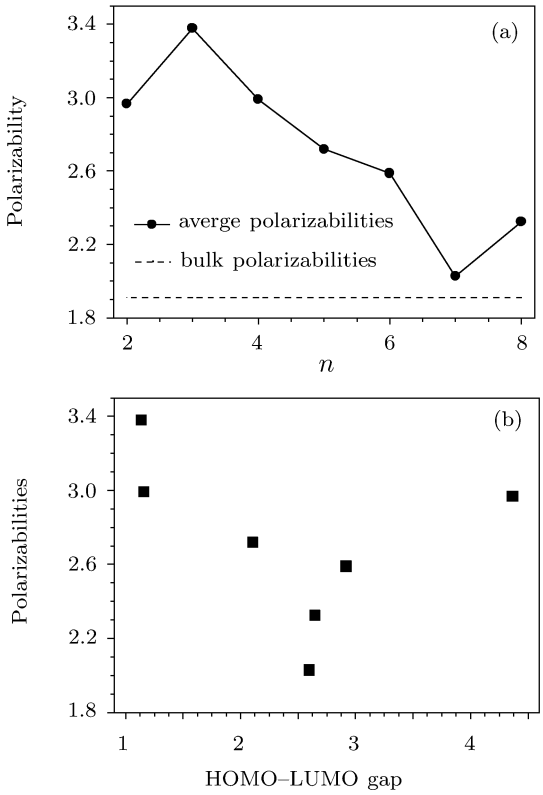


Fig.4. (a) Average polarizabilities (Å^3/atom) per atom of S_n clusters versus cluster size. The dashed lines correspond to the bulk polarizabilities (Å^3/atom) calculated according to Eq.(3). (b) Polarizabilities (Å^3/atom) of S_n clusters plotted against the HOMO–LUMO gap (eV).

Moreover, the polarizabilities of the cluster are also closely related to geometrical characteristics. For example, the HOMO–LUMO gap of S_6 is larger than that of S_7, while the polarizability of the former is larger than that of the latter. This can be attributed to their structural difference. For S_5, the structure is boat-shaped with C_{2V} symmetry, while S_7 is chair-shaped with C_s symmetry. The compact structures have relatively less and shorter bonds, which leads to the valence-electron binding tighter. Thus, a smaller volume is obtained in the compact structure, which causes a smaller polarizability for S_7.

4. Conclusion

In conclusion, we have performed the first principles calculation of the absorption spectra of bare S_n clusters, in their ground-state geometry, using the

TDLDA formalism. It may allow for a comparison with future experimental investigations. The TDLDA spectra display a significant blue shift with respect to the LDA spectra. The calculated spectra present a variety of features that could be used for cluster identification. We have found that the TDLDA-computed spectra differ significantly from those computed using a simple LDA approach, in both absorption threshold and spectral features. We also obtain a significant threshold absorption, which can distinguish between different ground states of the sulfur clusters.

Moreover, we have implemented a real-space *ab initio* computational technique to calculate polarizabilities of small S_n clusters. Our calculations indicate that in all the cases considered the polarizabilities are higher than the values estimated from the 'hard sphere' model with the bulk static dielectric constant. This work represents the first systematic theoretical study for the polarizabilities of semiconductor clusters. The polarizabilities decrease with the increase of the HOMO–LUMO gap as a whole. The polarizabilities are closely related to the HOMO–LUMO gaps and the geometrical configurations.

References

[1] Donohue J 1974 *The Structures of the Elements* (New York: Wiley) Chapter 9

[2] Steudel R 1984 *Studies in Inorganic Chemistry* ed Muller A and Krebs B (Amsterdam: Elsevier) p3

[3] Martin T P 1984 *J. Chem. Phys.* **81** 4427

[4] Chelikowsky J R and Louie S G 1996 *Quantum Theory of Real Materials* (Boston, MA: Kluwer)

[5] Honea E C, Ogura A, Murray C A, Raghavachari K, Sprenger O, Jarrold M F and Brown W L 1993 *Nature* **366** 42

[6] Cheshnovsky J R, Yang S H, Pettiette C L, Craycraft M J, Liu Y and Smalley R E 1987 *Chem. Phys. Lett.* **138** 119

[7] Sumathi K and Balasubramanian K 1992 *Chem. Phys. Lett.* **193** 251

[8] Li B X and Cao P L 2000 *Phys. Rev.* B **62** 15

[9] Lu Z Y, Wang C Z and Ho K M 2000 *Phys. Rev.* B **61** 2329

[10] Grigoryan V G and Springborg M 2001 *Phys. Chem. Chem. Phys.* **3** 5135

[11] Doye J P K and Wales D J 1998 *New J. Chem.* **1998** 733

[12] Wang J L, Zhao J J, Ding F, Shen W F, Lee H and Wang G H 2001 *Solid State Commun.* **117** 593

[13] He C L ,Wang F and Li J M 2003 *Acta Phys. Sin.* **52** 1297 (in Chinese)

[14] Jia W H and Wu H S 2004 *Acta Phys. Sin.* **53** 84 (in Chinese)

[15] Li E L ,Yang C J ,Chen G C ,Wang X W and Ma D M 2005 *Acta Phys. Sin.* **54** 4117 (in Chinese)

[16] Zhao J J, Wang J L and Wang G H 1993 *Phys. Lett.* A **275** 281

[17] Bai Y L, Chen X R,Yang X D and Zhou X L 2003 *J. Phys.* B: *At. Mol. Opt. Phys.* **36** 4511

[18] Chen X R, Oshiyama A and Okada S 2003 *Phys. Rev.* B **67** 033408

[19] Chen X R, Oshiyama A, Okada S and Gou Q Q 2003 *Chin. Phys. Lett.* **20** 404

[20] Blanc J, Bonaěić-Koutecký V, Broyer M, Chevaleyre J, Dugourd P, Koutecký J, Scheuch C, Wolf J P and Wöste L 1992 *J. Chem. Phys.* **96** 1793

[21] Wang C R C, Pollack S, Cameron D and Kappes M M 1990 *J. Chem. Phys.* **93** 3787

[22] Rinnen K D and Mandich M L 1992 *Phys. Rev. Lett.* **69** 1823

[23] Schafer R and Becker J A 1996 *Phys. Rev.* B **54** 10296

[24] Buenker R J, Peyerimhoff S D and Butscher W 1978 *Mol. Phys.* **35** 771

[25] Rohlfing M and Louie S G 1998 *Phys. Rev. Lett.* **81** 2312

[26] Casida M E 1995 *Recent Advances in Density-Functional Methods* (Part I) ed Chong D P (Singapore: World Scientific) p155
Casida M E 1996 *Recent Developments and Applications of Modern Density Functional Theory* ed Seminario J M (Amsterdam: Elsevier) p 391

[27] Vasiliev I, Öğüt S and Chelikowsky J R 1999 *Phys. Rev. Lett.* **82** 1919

[28] Vasiliev I, Öğüt S and Chelikowsky J R 1999 *Phys. Rev.* B **60** 8477

[29] Vasiliev I, Öğüt S and Chelikowsky J R 2000 *Cluster and Nanostructure Interfaces* ed Jena P, Khanna S N and Rao B K (Singapore: World Scientific) p259

[30] Chelikowsky J R, Troullier N, Wu K and Saad Y 1994 *Phys. Rev.* B **50** 11355
Chelikowsky J R, Troullier N, Jing X, Dean D, Binggeli N, Wu K and Saad Y 1995 *Comput. Phys. Commun.* **85** 325

[31] Ceperley D M and Alder B J 1980 *Phys. Rev. Lett.* **45** 566

[32] Troullier N and Martins J L 1991 *Phys. Rev.* B **43** 1993

[33] Blasé X, Rubio A, Louie S G and Cohen M L 1995 *Phys. Rev.* B **52** R2225

[34] Kurtz H A, Stewart J J P and Dieter K M 1990 *J. Comp. Chem.* **11** 82

[35] Quong A A and Pederson M R 1992 *Phys. Rev.* B **46** 12906
Quong A A and Pederson M R *Phys. Rev.* B **46** 13584

[36] Vasiliev I, Öğüt S and Chelikowsky J R 2001 *Phys. Rev. Lett.* **86** 1813

[37] Troparevsky M C, Kronik L and Chelikowsky J R 2002 *Phys. Rev.* B **65** 033311

[38] Lupinetti C and Thakkar A J 2005 *J. Chem. Phys.* **122** 044301

[39] Kuzyk M G and Dirk C W 1990 *Phys. Rev.* A **41** 5098